6-2022

Expression and purification of the bacterial protein Curli CsgA and its cross-interactions with amyloid-B

Leah Grace Cantrell
The University of Southern Mississippi

Expression and purification of the bacterial protein Curli CsgA and its cross-interactions with amyloid-β

by

Leah Grace Cantrelle

A Thesis
Submitted to the Honors College of
The University of Southern Mississippi
in Partial Fulfillment
of Honors Requirements

May 2022

Approved by:

Vijay Rangachari, Ph.D., Thesis Advisor,
School of Mathematics and Natural Sciences

Bernd Schroeder, Ph.D., Director,
School of Mathematics and Natural Sciences

Sabine Heinhorst, Ph.D., Dean
Honors College

ABSTRACT

One of the main causes of neurodegenerative diseases is aggregation of amyloid proteins that are toxic to the neurons. Proteins like amyloid-β (Aβ) and α-syneuclein (α-syn) form hallmark aggregate lesions that contribute to pathological processes in the brain in Alzheimer and Parkinson's patients, respectively. Recent ground-breaking studies have suggested a link between the microbiota of the gut and neurodegenerative diseases, called the "gut-brain axis." It has been long known that the protein, CsgA found in many enteric bacteria, forms amyloid fibers of its own called Curli. Curli fibrils are a structural component of bacterial colonies and maintain the integrity of biofilms, making CsgA a "functional amyloid protein." In this study, the hypothesis that CsgA and Aβ interact directly with one another to support the suggestion of the gut-brain axis is investigated. To do so, a plasmid containing CsgA is recombinantly expressed in *E. coli* cells and then purified in large scales for further testing of its interactions in-vitro. Various biophysical methods were used to isolate the CsgA protein in pure form. Once isolated, the interactions of CsgA with Aβ and other extracellular components reveal that CsgA inhibits the aggregation of Aβ, but Aβ seems to have no effect on the aggregation of CsgA. CsgA aggregation was also observed to be unaffected by the presence of NaCl.

Keywords: protein aggregation, neurodegenerative disease, brain-gut axis, amyloid-β, Curli

ACKNOWLEDGMENTS

I would not have been able to successfully graduate from the Honors College if Dr. Vijay Rangachari had not offered me an undergraduate position in his research lab. Being a biology major, I thought it was a shot in the dark to ask to join his biochemistry lab. However, just from taking his online Biochemistry I course, I could tell that he cares greatly about the education and experience of all students. I could not have imagined a better research experience, and I am immensely grateful that he went out of his way to mentor me this past year. The lab environment and culture between Dr. Rangachari and his students, both graduate and undergraduate, has been both a pleasure and a privilege to be able to experience.

I would also like to acknowledge my graduate mentor Jhinuk Saha for taking on an additional project and guiding me through this process. Starting from zero research experience, except for the supplemental lab courses of my biology degree, there were many times when certain things just would not click, but Jhinuk remained patient and explained everything until I understood. Without Jhinuk's guidance, I would have not gained the confidence in research that I now have. I am tremendously thankful for her patience, guidance, and knowledge.

Finally, I would like to thank the Honors College of The University of Southern Mississippi for granting me these experiences. At first, joining as a Keystone scholar made me worry that I would fall short of the experiences and knowledge compared to those who joined their freshman year; however, I grew close to many of those students and have enjoyed working with these peers as we conclude our undergraduate journey.

The privilege of being an Honors Scholar has afforded me growth in many skills and abilities that I will carry with me beyond graduation.

TABLE OF CONTENTS

LIST OF ILLUSTRATIONS

LIST OF ABBREVIATIONS

AD	Alzheimer disease
Aβ	Amyloid-β protein
α-syn	α-syneuclein protein
PD	Parkinson's disease
HPLC	high performance liquid chromatography
OD	optical density
IPTG	isopropyl b-D1-thiogalactopyranoside
SDS PAGE	sodium dodecyl sulfate-polyacrylamide gel electrophoresis
MALDI	matrix assisted laser desorption/ionization
SA	sinapinic acid
ThT	thioflavin-T
MWCO	molecular weight cut off
CD	circular dichroism

CHAPTER I: INTRODUCTION

1.1 Neurodegenerative diseases and the brain-gut axis

Neurodegenerative diseases are described as diseases that affect the central nervous system and drive cognitive decline of victims in late adulthood. Of the several types of neurodegenerative diseases, Alzheimer disease (AD) is the most common, leading to neuronal decline that results in fatality.[1] One of the hallmark lesions of AD is the presence of extracellular aggregates of amyloid-β protein (Aβ).[2] Aβ is an intrinsically disordered protein which is prone to abberant aggregation both without and upon interaction with multiple partners.[1]

Specifically, it has been found that low molecular weight aggregates of Aβ protein generated by anionic lipid micelles can drive neuronal decline in AD inflicted mice brains.[3] Aggregation of Aβ has also been influenced by another protein, α-synuclein (α-Syn), involved in Parkinson's disease (PD).[4] These reports indicate that multiple players are involved in AD-related neurodegeneration that potentially give rise to the onset of several phenotypes and clinical sub-types. While there are many existing hypotheses for various phenotypes in AD, one of the recent ones is the involvement of bacterial amyloids in interacting with proteins like α-Syn and Aβ leading to neurodegenerative diseases.[5, 6, 7]

Bacteria in human gut microbiomes are generally known to aid the digestive system in the breakdown of foods into nutrients that can be absorbed by the body. Interestingly enough, gut microbiota affect much more than the body's digestive system; they also affect the nervous system of the body, known as the gut-brain axis. The gut-brain axis was coined to acknowledge the steady, bidirectional communication that

occurs between the digestive tract and the central nervous system.[8] This communication is thought to occur by way of metabolic activity of endosymbiotic microbes in the gut: by-products of these microbes increase intestinal permeability allowing neurotransmitter production and absorption to be influenced by these gut processes.[8]

1.2 Curli CsgA

In bacterial cells such as *E. coli*, amyloid proteins are formed to help them produce biofilms as a method of protection against extracellular environmental factors; however, these amyloidogenic proteins can be transported to the brain through the gut-brain axis and modulate the aggregation of other proteins to initiate various neurodegenerative diseases.[5, 6] An interesting gut bacterial protein, CsgA, was discovered in the 1980s that displayed the ability to form amyloid fibrils called Curli that aid in biofilm formation.[9] There is a void in the knowledge of how exactly these protein aggregates form and interact with other cellular components of the body to induce toxicity and neurodegeneration.[10] This study is an ongoing research project that aims to further understand the Aβ aggregations induced by CsgA.To observe the interaction in-vitro among the aforementioned proteins, they needed to be recombinantly expressed within the bacterial cells and purified via various biochemical techniques in large scales.

1.3 Rationale and hypotheses

To uncover the mechanistic link between the gut microbiota and neurodegeneration, we hypothesize that CsgA amyloids cross-interact with Aβ that is also present in the intestines to promote toxic oligomers of the latter. While Aβ recombinant

expression and purification has been well-established in the laboratory, this project is focused on recombinant expression and purification of CsgA protein in *E. coli* cells. Once expressed and purified, the interactions and behaviors of CsgA under various conditions will be observed. It is hypothesized that CsgA will show some effect upon interactions with other amyloidogenic proteins such as Aβ and that aggregation of CsgA will be affected by interaction with other cellular components, providing evidence for the gut-brain axis.

CHAPTER II: MATERIALS AND METHODS

2.1 Materials

CsgA plasmid was a generous gift from Chapman lab at the University of Michigan. The C8 Zorbax semi-prep high performance liquid chromatography (HPLC) column was purchased from Agilent. Routine lab chemicals were purchased from Sigma-Aldrich and Thermofisher. BL21-DE3 and DH5α competent cells were grown and transformed with CsgA plasmid. Ni-NTA column was used in addition to Tris base, imidazole washes, guanidine hydrochloride, and strip buffer.

2.2 Methods

Plasmid Isolation from DH5α cells. A 2 µL aliquot of CsgA plasmid was added to 10 µL of DH5α competent cells and allowed to sit for 30 minutes at room temperature. The cells and plasmid were then heat-shocked for 20 seconds and immediately placed in ice for an additional two minutes. Next, 200 µL of SOC media was added to the mixture, and it was allowed to agitate for one hour at 37˚C. The cells were then plated in amounts of 125 µL (i), 50 µL (ii), and 25 µL (iii) and incubated overnight.

Colony numbers 1-6 were chosen and placed into media tubes containing 2 mL of LB ampicillin broth each. The tubes were left to incubate overnight for plasmid extraction the following day. The DH5α cells were centrifuged in 4-6 mL aliquots at 18,000 RCF for 2 minutes. The cell pellet was then resuspended in 600 mL of H_2O. 100 µL of Zymo 7x lysis buffer and 350 µL of neutralization buffer were added and mixed. The cell solution was centrifuged again at 13,000 RCF for 10 minutes, and the supernatant was added to the Zymo column. The Zymo column was placed in a collection

tube, centrifuged at 13,000 RCF for 1 minute, and the flow through was discarded. 200 µL of Eudo-wash buffer were added and then the Zymo column was centrifuged again for 1 minute. 400 µL of Zyppy wash buffer were added to the column next and centrifuged for 1 minute. The Zymo column was transferred to a clean Eppendorf tube and 20 µL of warm H_2O (~ 40˚C) were added to the column matrix and incubated at room temperature for 20 minutes. The tube was centrifuged for a last time at 10,000 RCF for 2 minutes to elute the DNA for imaging. The plasmid was stored at -20˚C for future use.

Transformation and growth of BL21-DE3 cells. A 2 µL aliquot of CsgA plasmid was added to 10 µL of BL21-DE3 competent cells and allowed to sit for 30 minutes at room temperature. The cells and plasmid were then heat-shocked for 20 seconds and immediately placed in ice for an additional two minutes. Then, 200 µL of SOC media were added to the mixture, and it was allowed to agitate for one hour at 37˚C. The cells were then plated on ampicillin agarose plates using sterile glass beads in amounts of 125 µL (i), 50 µL (ii), and 25 µL (iii) and incubated overnight at 37˚C. There were 2 sets of transformations performed: CsgA I (i, ii, iii) and CsgA II (i, ii, iii). An aliquot of the transformed BL21-DE3 cells were incubated overnight in 100 mL of LB media broth with 100 µL of Ampicillin at 37˚C in the shaker. The following day, 1 mL each of the overnight cell culture was added to two autoclaved flasks containing 1 L of LB broth media each. The flasks were then placed in the shaking incubator at 37˚C, and the optical density (OD) was recorded in 15-minute intervals. The cells in each flask were induced with 1 mL of isopropyl b-D1-thiogalactopyranoside (IPTG) once the OD reading measured between 0.6 and 0.8 OD600 and then left to incubate in the shaker at 37˚C overnight. The media was then added to four 500 mL containers, and the cells were

centrifuged for 20 minutes at 10,000 RCF. The supernatant was discarded and the containers with the remaining pellets were stored in the -20˚C freezer.

Ni(II)-affinity chromatography. Stored BL21-DE3 cells from the -20˚C were obtained in the amount of 1 L. The cells were resuspended in 50 mL of 20 mM Tris buffer + 1 mM EDTA (pH 7.2) and then sonicated for 12 cycles of 30 seconds on/1 minute off at 18/20 power. The sonicated cells were then centrifuged at 20,000 RCF for 20 minutes. The supernatant (supernatant I) from the centrifugation was discarded, and the pellet (pellet I) was resuspended in 6 M guanidine hydrochloride to lyse the inclusion bodies that contain the protein of interest. After resuspension, pellet I was sonicated again for 10 cycles of 30 seconds on/1 minute off at 18/20 power. The lysate of pellet I was centrifuged once more at 20,000 RCF for 20 minutes. The supernatant (supernatant II) was collected, and the pellet (pellet II) was discarded.

The Ni-NTA column was equilibrated with 10 mL of 200 mM $NiSO_4$ and 8 mL of guanidine hydrochloride. Supernatant II was added to the column containing Ni-NTA beads. The column was inverted several times to suspend the beads in the supernatant. The suspended Ni-NTA beads in supernatant II were allowed to mix overnight at 4˚C on a shaker to allow the 6 His-tag of CsgA to bind to the Ni(II) in the beads. The next day, supernatant II containing the Ni-NTA beads was run through the column, and the flow-through was collected. The column was then washed with 50 mL of 20 mM Tris buffer (pH 7.2) to wash out any unbound contaminants. Washes of 50 mL of 50 mM imidazole and 30 mL of 100 mM imidazole were run to wash out any non-specifically bound proteins. To elute the protein of interest, 6 mL of 300mM imidazole were run through the column to cleave the bond between the protein and the Ni-NTA beads. The 6 mL elution

was added to clean Eppendorf tubes in 1 mL aliquots each and stored in the -80˚C freezer.

High Performance Liquid Chromatography (HPLC). The C18 Phenomenex semi-prep HPLC column was prepped and equilibrated with 95% nanopure H_2O and 5% acetonitrile containing 0.01% TFA. Equilibrated column was heated to ~ 60˚C and a 1 mL aliquot of CsgA (500 mL/6) was loaded to the HPLC column. HPLC purification was done at 60˚C with increasing acetonitrile gradient. Protein samples were collected in acetonitrile-water and further characterized and lyophilized for later use.

Gel electrophoresis and immunoblotting. Prior to sodium dodecyl sulfate-polyacrylamide gel electrophoresis (SDS PAGE), 1X Laemmli loading buffer (1% SDS) was added to the samples before loading them into 4%-20% Bis-Tris Bio-Rad TGX gels without heating. For fragment molecular weight comparison, pre-stained molecular weight markers (Novex Sharp Protein Standard, Life Technologies) were run in parallel. Following PAGE, gels were immunoblotted onto a 0.2 μM nitrocellulose membrane (Bio-Rad) and boiled in 1X PBS in a microwave oven for 1 minute. The immunoblot was then blocked in 1X PBS containing 5% nonfat dry milk and 1% Tween 20 for 1.5 hours at 25 ºC before being probed overnight with Aβ-specific Ab5 monoclonal antibody (1:6000 dilution) at 4 ºC. Anti-mouse, horseradish peroxidase-conjugated secondary antibody (1:6000 dilution) was then used to probe the immunoblot for 1.5 hours at 25 ºC. Blots were then imaged with a Super SignalTM West Pico Chemiluminescent Substrate kit (Thermo Fisher Scientific).

MALDI-MS spectroscopy. The Bruker Daltonics Microflex LT/SH TOF-MS system was used for matrix assisted laser desorption/ionization (MALDI) mass

spectrometry. The system was calibrated using the Bruker Protein Calibration Standard I (Bruker Daltonics). A 2 μL aliquot of sinapinic acid (SA) matrix in saturated AcN and H_2O and a 2 μL aliquot of HPLC fraction 21 were added to a clean Eppendorf tube and mixed well. The 4 μL solution was then spotted onto a Bruker MSP 96 MicroScout Target with plate and allowed to dry at 37˚C for 15 minutes before collecting spectra.

Circular dichroism (CD) spectroscopy. A Jasco J-815 spectropolarimeter was used to collect UV CD spectra of 10-25 μM of CsgA at 260-190 nm. An aliquot of CsgA protein was added to a 1 mm pathlength quartz cuvette and 6-16 UV scans were conducted at 50 nm/min with an 8 second response time, 1 nm bandwidth, and 0.1 nm data pitch. The Jasco spectrum analysis program was used to average the data from each spectral scan for analysis.

Aggregation of CsgA. Aggregation kinetics of CsgA was monitored by thioflavin-T (ThT) fluorescence at 37 º C in a BioTek Synergy 96 well plate reader. The reactions with CsgA were carried out with Aβ monomer (10 μM) and various concentrations of CsgA in the presence of 50 mM NaCl & 50 μM ThT in 20mM Tris buffer (pH 8.0). Each reaction was transferred in 200 μL aliquots to a Corning 96-well plate (black plates) for aggregation kinetics. Samples were excited at 452 nm, and ThT fluorescence was obtained with an emission at 485 nm at every 10 minutes at 37ºC with shaking.

CHAPTER III: RESULTS

3.1 Plasmid isolation from DH5α cells

The concentration of the extracted plasmid was measured on a nanodrop as 151.9 ng/µL with 1.81 A_{260}/A_{280}, and 1.78 A_{260}/A_{230}. The extracted plasmid was stored in the -20˚C freezer for further use.

3.2 Transformation of BL21DE3 cells

After overnight incubation of the two sets of transformations, well-isolated colonies of cells were selected (Fig. 1), labelled, and streaked on second agar plates, and stored at 4˚C for further use.

Figure 1: A plate of ampicillin-containing CsgA BL21-DE3 cells is shown. Colonies are marked for picking on the underside of the plate.

3.3 Expression of CsgA colonies

Cell stocks were made from the colonies and the expression levels of the protein were analyzed. The cells were lysed and loaded on to a 10% tris-glycine gel for electrophoresis. The gels developed by silver stain techniques indicated that all colonies between 13-22 expressed the CsgA protein as indicated by the band in each lane at 14 kDa (Fig. 2).

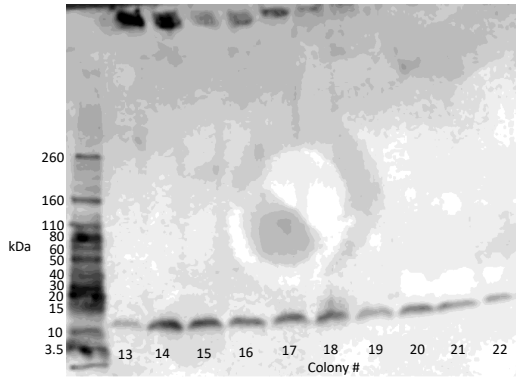

Figure 2: The SDS PAGE gel shows the silver stain of the expression check of the plasmid.

3.4 Optimized Purification of CsgA

The purification protocol involving the lysis of the inclusion bodies via a second resuspension and sonication from the pellet obtained from the initial centrifugation was optimal for CsgA purification yield. Gels developed with silver stain techniques revealed a band at 14 kDa in the 300 mM lane (Fig. 3), indicating the presence of CsgA with minimal contaminants as well as minimal protein elution in the following lane labelled "S" containing the strip buffer.

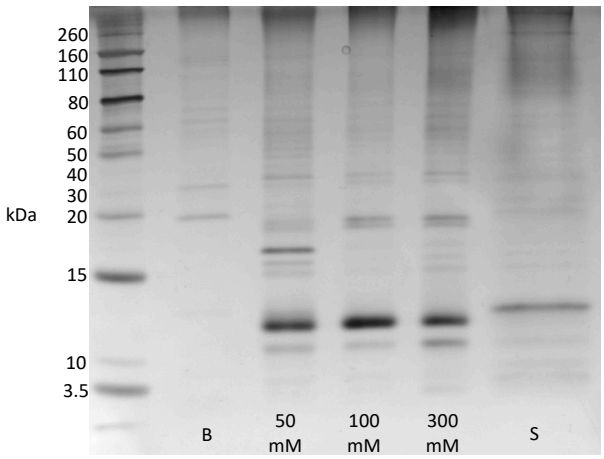

Figure 3: This image shows an SDS PAGE gel from the final optimized purification protocol developed with silver stain.

3.5 Purification Troubleshooting Processes

Use of SpinTrap G-25 desalting columns. The initial purification protocol for CsgA involved resuspending the stored cells in 6 M guanidine hydrochloride, sonicating the resuspended cells, collecting the supernatant, and discarding the pellet. The supernatant was allowed to mix with the Ni-NTA beads for 1 hour at 4˚C before being

run through the Ni-NTA column. When the UV absorbance of the protein was observed, a peak at 250 nm instead of 280 nm suggested that the protein may have precipitated or was strongly bound to DNA (Fig. 4). This initial method of purification yielded a very small concentration of protein (196 µg/L of cells) even after desalting the 200 mM eluate with SpinTrap G-25 desalting columns.

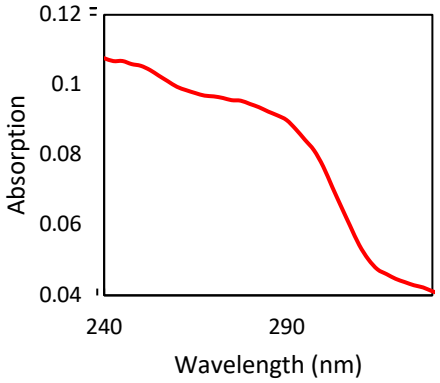

Figure 4: This graph of UV spectroscopy is representative of the initial purification methods using desalting methods. A peak at 250 nm instead of 280 nm (indicative of CsgA) is observed.

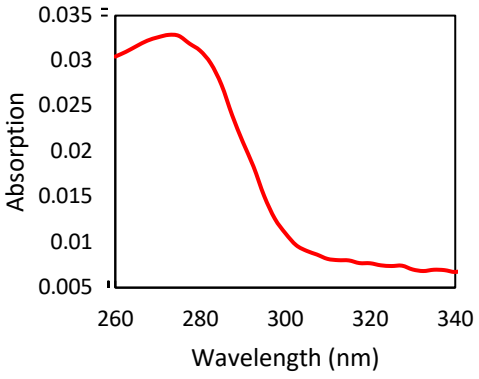

Figure 5: This graph of UV spectroscopy is representative of early purification methods using a 10 kDa Amicon Ultra centrifugal filter. A peak at 275 nm instead of 280 nm (indicative of CsgA) is observed.

Use of 10 kDa Amicon Ultra MWCO filter. Later modifications of the purification protocol added filtration of the elution through a 10 kDa Amicon Ultra molecular weight cut off (MWCO) centrifugal filter. The Ni-NTA column was washed with 10 mL of 200 mM imidazole buffer to elute the Ni-NTA bound protein. The eluate was added to a 30 kDa Amicon Ultra MWCO centrifugal filter to remove any remaining tags that were bound to the protein. A 10 kDa Amicon Ultra MWCO centrifugal filter was subsequently used to remove any smaller fragment residues. The protein was then dialyzed with 20 mM Tris buffer (pH 7.2) using an 8 kDa membrane. When the UV absorbance of the protein was

imaged (Fig. 5), a peak at 275 nm was observed, and visible precipitate was observed on the Amicon filter after centrifugation. The calculated concentration of protein increased from the previous protocol (460 µg/L of cells); however, it was still lower than optimal for use in further experiments. The SDS PAGE gel developed with silver stain (Fig. 6) showed a prominent band just at 14 kDa in the 10 kDa lane suggesting presence of CsgA protein; other bands suggest the presence of higher molecular weight aggregates and other non-specifically Ni-NTA bound proteins that eluted with the 200 mM elution.

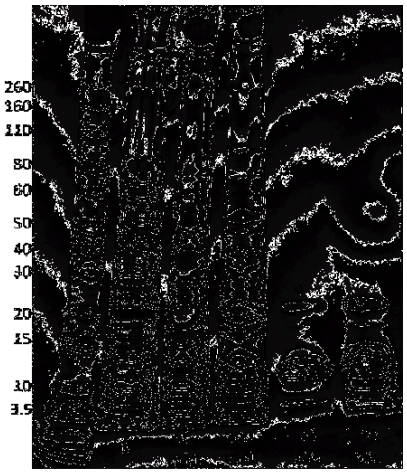

Figure 6: This SDS PAGE gel developed with silver stain represents the modified purification protocol that utilizes a 10 kDa Amicon Ultra MWCO centrifugal filter.

Lysing of inclusion bodies. When the UV absorbance of the protein was observed (Fig. 7) following purification using techniques to lyse inclusion bodies, a peak was seen at 280 nm, and the calculated protein concentration yield (892.8 µg/L of cells) was almost doubled from the previous protocol. Gel electrophoresis run on the purifications that lysed the inclusion bodies were run and stained with silver stain techniques. In the lane labelled "E"

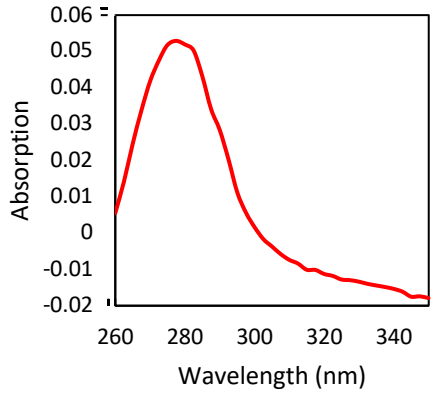

Figure 7: This graph of UV spectroscopy is representative of the optimized purification protocol that allowed for the lysis of inclusion bodies. The peak at 280 nm is indicative of the presence of CsgA.

for final elution in 300 mM imidazole wash (Fig. 8), a band at 14 kDa is observed that represents the elution of the CsgA protein. It can also be observed that some contaminants were eluted in the 50 mM imidazole wash lane contributing to the successful final elution of protein.

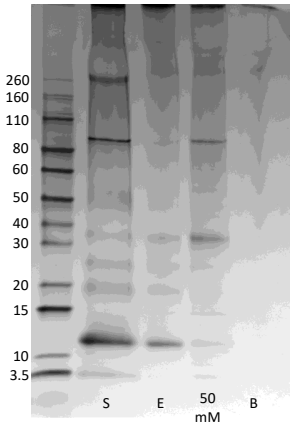

Figure 8: This SDS-PAGE gel is one of many developed with silver staining techniques that depict CsgA protein yield in the second lane labelled "E" for elution in 300 mM imidazole wash.

3.6 Confirmation of CsgA Purification

After collecting the elution sample from the optimized purification protocol, HPLC was run (Fig. 9) and an SDS PAGE gel was developed with silver stain in which the band at 14 kDa in the fraction 21 (F21) lane corresponds to the presence of CsgA (Fig 10). A dot blot (Fig. 11) and MALDI mass spectrometry (Fig. 12) were performed on HPLC fractions 21, 22, and 23. Analysis of the mass spectrometry data from HPLC fractions 21, 23, and 23 revealed that fraction 21 contained the protein of interest indicated by the peak with the molecular weight just under 4,000 kDa (Fig. 12). HPLC

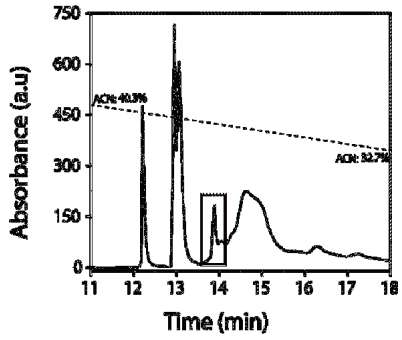

Figure 9: In this HPLC graph, the peak at 14 minutes indicates the peak for fraction 21.

Figure 10: In this HPLC SDS PAGE gel developed with silver stain, the band at 14 kDa in fraction 21 (F21) indicates the presence of CsgA.

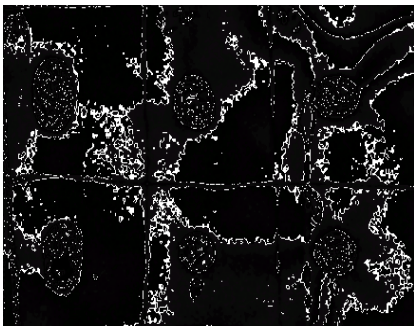

Figure 11: This image depicts the dot blot of HPLC fractions 21, 22, and 23.

fraction 21 was calculated to contain 13.9 kDa of CsgA protein. Fraction 21 was then lyophilized in cold lyophilizer and resuspended in 20 mM Tris buffer (pH 7.2).

Biophysical characterization. Circular dichroism (CD) of HPLC fraction 21 revealed that the protein possessed a random coil structure indicated by a minima peak at 200 nm (Fig. 13). ThT (Thioflavin-T) fluorescence analysis was done to analyze the aggregation of CsgA, as it is known to form amyloids. Therefore, 25 µM of protein both with and without the presence of NaCl were analyzed at 37 º C. CsgA

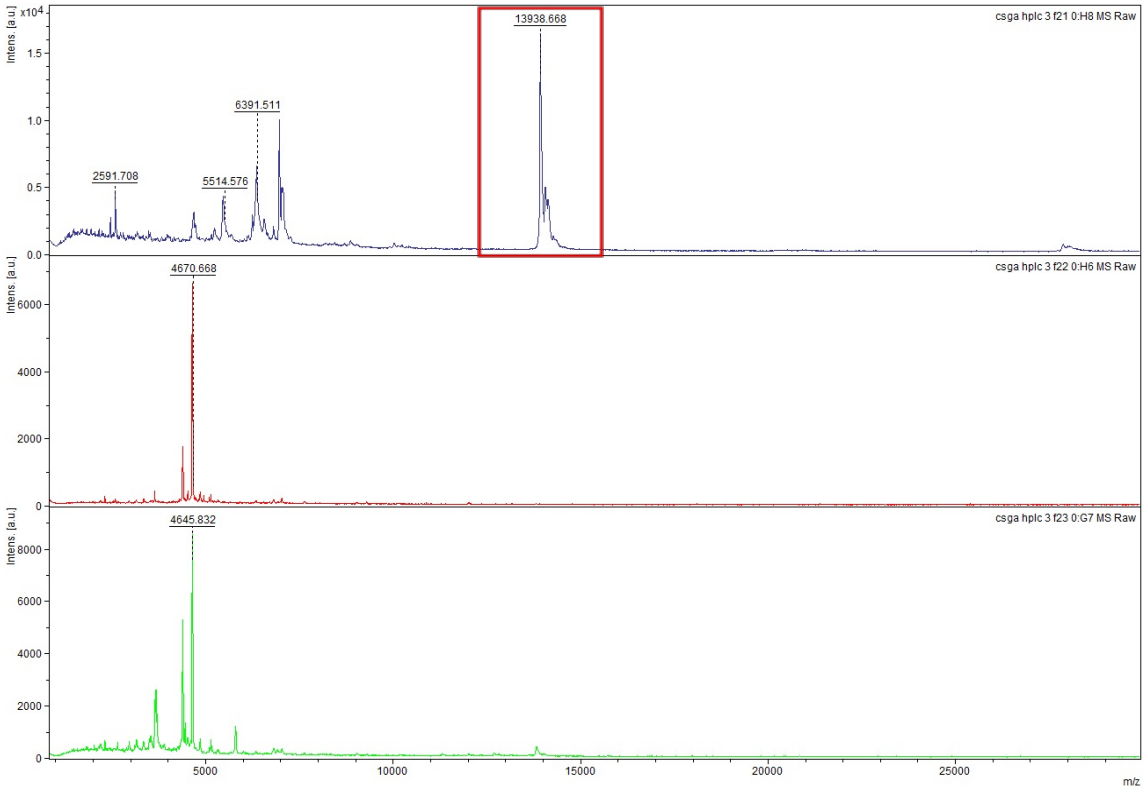

Figure 12: In this figure, mass spectrometry peaks of HPLC fraction 21, 22, and 23 are shown. The blue peak indicates the molecular weight of fraction 21 at 13,938.668 kDa.

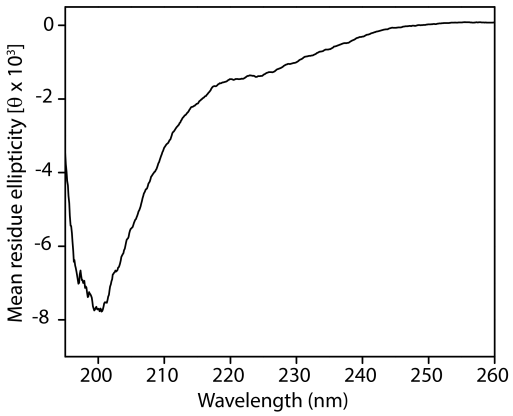

Figure 13: This graph of CD data shows a minima at 200 nm indicating that CsgA has a random coil structure.

aggregation over a period of 24 hours was recorded and revealed that the protein aggregates both with and without NaCl at approximately the same rate with no significant difference (Fig. 14). Finally, the interaction of CsgA with Aβ protein was also observed analyzing ThT fluorescence and gel electrophoresis on the co-incubations of the two proteins at different stoichiometries (Fig. 15). As expected, it was observed that Aβ begins aggregation at around the 10-hour mark (blue triangles; Fig. 15). Notably, the presence of CsgA inhibits the aggregation of Aβ in all stochiometries. The CsgA control showed no aggregation within the experimental time frame. These data suggest a strong influence of CsgA on Aβ aggregation and provides a molecular foundation for the effect of bacteria on AD.

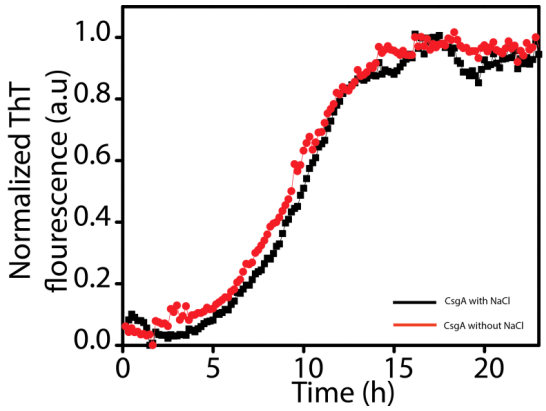

Figure 14: This ThT (Thioflavin-T fluorescence) graph shows aggregation of CsgA both with (black) and without (red) the presence of NaCl.

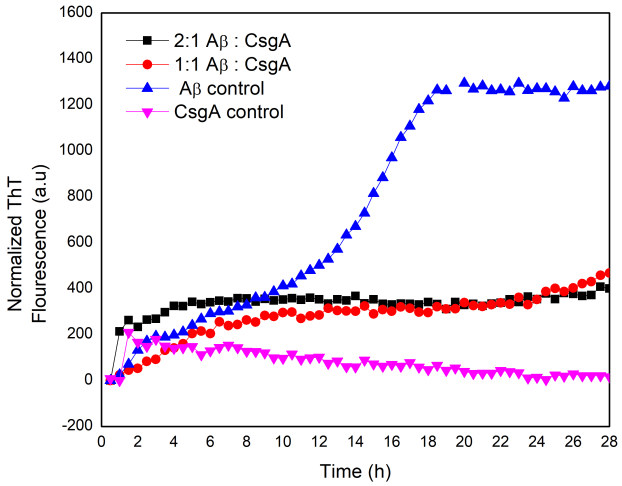

Figure 15: ThT fluorescence data on the interaction between CsgA with Aβ and how their aggregation is affected. Aβ was kept constant at 10 µM while 5 and 10 µM CsgA was used. The control CsgA corresponds to 10 µM.

CHAPTER IV: DISCUSSION AND CONCLUSION

Protein aggregation of amyloidogenic proteins is becoming increasingly relevant as one of the hallmarks of neurodegenerative diseases. There is also growing evidence of interactions between proteins of the gut microbiome and amyloidogenic neuronal proteins via interplay between metabolic byproducts of symbiotic gut microbiomes and influence on neurotransmitters. Throughout the course of this project, Curli fibril forming CsgA protein purification protocol was standardized with intentions of isolating the protein to observe its interactions with other amyloidogenic proteins and biophysical components. The standardized purification process was time-consuming, as initial purifications yielded insignificant amounts of impure protein. Each unsuccessful purification provided further insight to how the protocol could be optimally modified. Through Ni(II)-affinity purification with an Ni-NTA column and HPLC, purified CsgA was able to be obtained in amounts substantial enough for testing with ThT fluorescence and CD spectroscopy in the presence of NaCl and Aβ protein.

CD observations of CsgA revealed that the protein assumed a random coil structure after aggregation over 24 hours. CsgA was seen to aggregate in the presence of NaCl. Observations of ThT fluorescence of CsgA in the presence of and without NaCl revealed that NaCl had no significant effect on CsgA aggregation. The aggregation time remained relatively the same. However, when ThT fluorescence was observed for the interactions between Aβ and CsgA, significant results were presented. The CsgA control showed no signs of aggregation. The Aβ control was seen to begin aggregation around 10 hours, but in the presence of CsgA, Aβ did not aggregate. The CsgA amino acid sequence contains 10 negatively charged residues at pH 7.2, and the Aβ amino acid sequence

contains 6 negatively charged residues along with a large dissemination of hydrophobic residues that are involved in its aggregation. It is hypothesized that the repulsions between the proteins' negatively charged molecules interfere with the ability of Aβ to aggregate via the synergistic interactions between its negatively charged residues and hydrophobic residues. Further approaches to this study could use biophysical methods to investigate and test this hypothesis further.

Largely developing evidence of gut microbiota being linked to neurodegenerative diseases emphasizes further implications for studies of CsgA and its interactions with amyloidogenic neuronal proteins like Aβ. Knowing how proteins like CsgA interact with other biophysical components to induce neurodegeneration contribute to understanding, treatment, and prevention of neurodegenerative diseases. Studies like these provide further evidence of the gut-brain axis and can ultimately provide insight into just how influential gut microbiomes are on other essential parts of the body.

REFERENCES

(1) Rangachari, V., Dean, D. N., Rana, P., Vaidya, A., & Ghosh, P. (2018). Cause and consequence of AB – lipid interactions in alzheimer disease pathogenesis. *Biochimica Et Biophysica Acta (BBA) - Biomembranes*, *1860*(9), 1652–1662. https://doi.org/10.1016/j.bbamem.2018.03.004

(2) Ghosh, P., Kumar, A., Datta, B., & Rangachari, V. (2010). Dynamics of protofibril elongation and association involved in AB42 peptide aggregation in alzheimer's disease. *BMC Bioinformatics*, *11*(S6). https://doi.org/10.1186/1471-2105-11-s6-s24

(3) Saha J, Dean DN, Dhakal S, Stockmal KA, Morgan SE, Dillon KD, Adamo MF, Levites Y, Rangachari V. 2021. Biophysical characteristics of lipid-induced Aβ oligomers correlate to distinctive phenotypes in transgenic mice. The FASEB Journal. 35(2). doi:10.1096/fj.202002025rr.

(4) Dhakal S, Wyant CE, George HE, Morgan SE, Rangachari V. Prion-like C-terminal domain of TDP-43 and α-synuclein interact synergistically to generate neurotoxic hybrid fibrils. 2020. doi:10.1101/2020.12.12.422524

(5) Kowalski, K., & Mulak, A. (2019). Brain-gut-microbiota axis in alzheimer's disease. *Journal of Neurogastroenterology and Motility*, *25*(1), 48–60. https://doi.org/10.5056/jnm18087

(6) Sampson TR, Challis C, Jain N, Moiseyenko A, Ladinsky MS, Shastri GG, Thron T, Needham BD, Horvath I, Debelius JW, et al. A gut bacterial amyloid promotes α-

synuclein aggregation and motor impairment in mice. eLife. 2020;9. doi:10.7554/elife.53111

(7) Friedland RP, McMillan JD, Kurlawala Z. What are the molecular mechanisms by which functional bacterial amyloids influence amyloid beta deposition and neuroinflammation in neurodegenerative disorders? International Journal of Molecular Sciences. 2020;21(5):1652. doi:10.3390/ijms21051652

(8) de J.R. De-Paula, V., Forlenza, A. S., & Forlenza, O. V. (2018). Relevance of gutmicrobiota in cognition, behaviour and alzheimer's disease. *Pharmacological Research*, *136*, 29–34. https://doi.org/10.1016/j.phrs.2018.07.007

(9) Barnhart MM, Chapman MR. Curli biogenesis and function. Annual Review of Microbiology. 2006;60(1):131–147. doi:10.1146/annurev.micro.60.080805.142106

(10) Perov, S., Lidor, O., Salinas, N., Golan, N., Tayeb-Fligelman, E., Deshmukh, M., Willbold, D., & Landau, M. (2018). Structural insights into curli CsgA Cross-β fibril architecture inspired repurposing of anti-amyloid compounds as anti-biofilm agents. *PLOS*. https://doi.org/10.1101/493668